Gharamti, I. E.; Ahmad, W.; Puolakka, O.; Tuhkuri, J.

Thickness-independent fracture in columnar freshwater ice : An experimental study

Published in:
Engineering Fracture Mechanics

DOI:
10.1016/j.engfracmech.2024.109906

Published: 08/03/2024

Document Version
Publisher's PDF, also known as Version of record

Engineering Fracture Mechanics 298 (2024) 109906

Contents lists available at ScienceDirect

Engineering Fracture Mechanics

journal homepage: www.elsevier.com/locate/engfracmech

Thickness-independent fracture in columnar freshwater ice: An experimental study

I.E. Gharamti [a,b,*], W. Ahmad [a], O. Puolakka [a], J. Tuhkuri [a]

[a] *Department of Mechanical Engineering, Aalto University, Espoo, Finland*
[b] *VTT Technical Research Centre of Finland Ltd, Espoo, Finland*

ARTICLE INFO

Keywords:
Freshwater ice
Fracture
Thickness
Rate effect

ABSTRACT

Experiments on columnar freshwater ice indicated that there is no detected effect of the ice thickness on the fracture behavior of columnar freshwater S2 ice. The influence of thickness was studied using large laboratory-grown samples. Two series of Mode I fracture tests were carried out using deeply edge-cracked 3-by-6-metre rectangular plates loaded monotonically at 1…100 μm/s. The ice was warm (above −0.5 °C), and the ice thickness varied in the range 10–40 cm. This paper analyzes the second series of tests and compares the results with the first series tests; the analysis of the latter was published in Gharamti et al. (2021) [2,3,4]. The viscoelastic fictitious crack model (VFCM) was applied to analyze the data and calculate the crack profile, fracture energy and the process zone size. The thickness affected only and linearly the values of the measured loads with no influence on the fracture properties: the apparent fracture toughness, fracture energy, crack opening displacements, notch sensitivity and process zone size.

1. Introduction

When ice interacts with a structure, it exerts loads that are related to the failure process of ice. Depending on the prevailing conditions, ice properties (temperature, thickness, salinity, orientation, first-year vs. multi-year), structure geometry and dimensions (diameter, width, inclination) and the relative speed between ice and structure, ice can fail by crushing, buckling, bending, or splitting [1]. Ice failure is a complex process of multiple failure mechanisms rather than a single event. Splitting (fracture) under Mode I is common in many ice-engineering applications and is the focus of this study. It is crucial to find the relationship among various factors that influence the fracture process. Theoretical analysis is a challenging approach because ice is a quasi-brittle, viscous and anisotropic material. Most of the relations provided in the literature are empirical, based on experimental measurements and observations. The effects of several factors – scale, loading rate, temperature, notch acuity, grain size – on the fracture of freshwater ice have been studied extensively in the literature [2–10,10–21].

An interesting yet unaddressed question is the effect of the ice thickness (thickness of level ice or the consolidated layer of a ridge) on the fracture behavior. In fracture terminology, the ice thickness, i.e. the specimen thickness, is the length of the crack front. For the splitting fracture of metals, it is known that the state of stress near the tip of a crack tends to change from plane strain to plane stress as the ratio of width-to-thickness of a plate increases [22]. However, thickness has been shown not to affect the fracture of quasi-brittle materials such as concrete [23,24]. Ice is expected to behave as other quasi-brittle materials because a triaxial state of stress does not materialize; the tensile stress parallel to the crack front is assumed to be relieved by microcracking

* Corresponding author at: VTT Technical Research Centre of Finland Ltd, Espoo, Finland.
E-mail addresses: iman.elgharamti@aalto.fi, iman.elgharamti@vtt.fi (I.E. Gharamti), waqas.ahmad@aalto.fi (W. Ahmad), otto.puolakka@aalto.fi (O. Puolakka), jukka.tuhkuri@aalto.fi (J. Tuhkuri).

https://doi.org/10.1016/j.engfracmech.2024.109906
Received 11 September 2023; Received in revised form 29 January 2024; Accepted 29 January 2024
Available online 3 February 2024
0013-7944/

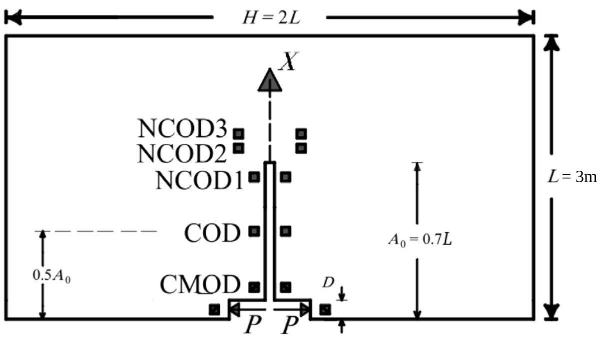

Fig. 1. Specimen geometry, edge cracked rectangular plate of length $L = 3$ m, width $H = 6$ m, and crack length $A_0 = 2.1$ m.

parallel to the top and bottom surfaces or by creep which takes place rapidly. No theoretical or experimental validation of this idea exists in the literature. It is important to study the thickness effect in a large-scale experimental program which varies the ice thickness. To the authors' knowledge, these kind of fracture experiments have not been conducted for ice.

The goal of the present study is to examine the quantitative influence of the ice thickness on the fracture behavior of columnar freshwater S2 ice. Two programs of Mode I large-scale fracture tests were conducted in the Ice and Wave Tank at Aalto University in 2017 and 2022. 3 m × 6 m deeply cracked edge-cracked rectangular plates (ECRP) were loaded monotonically with different control displacement rates (1…100 μm/s) under displacement control. Each initial notch was cut to be 70% of the plate dimension that is parallel to the crack. The ice sheet was warm (> −0.5°C). Details and results of the 2017 program were published in [2–4]. The thickness of the 2017 specimens was in the range 35–38 cm. During the 2022 test program, the parent ice sheet grew in thickness from 10 cm to 22 cm.

The experiments were analyzed by using the linear elastic fracture mechanics (LEFM) and the non-linear viscoelastic fictitious crack model (VFCM). The LEFM uses the weight function method, as formulated by Dempsey and Mu [25] and applied in [2], to calculate the apparent fracture toughness (K_Q). The VFCM approach, as formulated by Mulmule and Dempsey [26] and applied in [2], was implemented to derive the crack profile, fracture energy (G_f), and size of the fracture process zone (PZ).

The tests from 2017 and 2022 covered a thickness range of $h \approx 10-40$ cm. The results were analyzed for the effect of the thickness on the applied load and fracture parameters: the apparent fracture toughness, crack opening displacements, fracture energy, and size of the process zone.

Next, Section 2 presents a description of the experimental details. Section 3 briefly reviews the implementation of the LEFM and VFCM models. The results from 2017 and 2022 programs are summarized and discussed in Section 4. Section 5 concludes the paper.

2. Experimental details

Two 40 × 40-m sheets of columnar freshwater S2 ice were grown in the Ice and Wave Tank of Aalto University in 2017 and 2022. Edge-cracked rectangular plate (ECRP) samples, of length L (= 3 m) and width H (= $2L$), were cut and loaded at the crack mouth (Fig. 1). The ice thickness (h) of each ice sheet was constant. During the tests, the ice thickness of the 2017 ice sheet grew from ca. 35 cm to 40 cm, and the 2022 ice from ca. 10 cm to 22 cm. The grain size of the ice samples, i.e. average diameter of the columnar grains, was 3 mm at the top (2017 and 2022), 5 mm at the bottom of 20 cm thick ice (2022), and 10 mm at the bottom of 40 cm ice (2017). The ice temperature was warmer than −0.5°C; at the bottom of the ice sheet the ice temperature was 0°C. A long tip-sharpened edge crack of length A_0 ($A_0 \approx 0.7\ L$) was fabricated in each ice specimen.

The response of the ice at different positions along the crack was monitored by using surface-mounted linear variable differential transducers (LVDTs) (2017) and triangulation-based laser displacement sensors (2022); main locations are labeled in Fig. 1 as CMOD (at the crack mouth), COD (midway of the crack), NCOD1 (behind the tip), and NCOD2 and NCOD3 (ahead of the tip). A displacement-controlled actuator was inserted in the mouth of the pre-crack to monotonically load the specimen along a wide contact loading length D (Fig. 1) in order to avoid crushing at contact. The loading device was hydraulically operated in 2017 and electro-mechanically operated in 2022. The control displacement rates were in the range 1…100 μm/s. The global behavior of the crack propagation was straight extension to the far edge. A detailed description of the experimental setup, ice growth, temperature and grain profiles, and microstructural properties are provided in [2,3] for the earlier tests (2017). The new tests (2022) followed the same plan but with an updated loading device and instrumentation. The ice in the two programs exhibits similar properties and profiles.

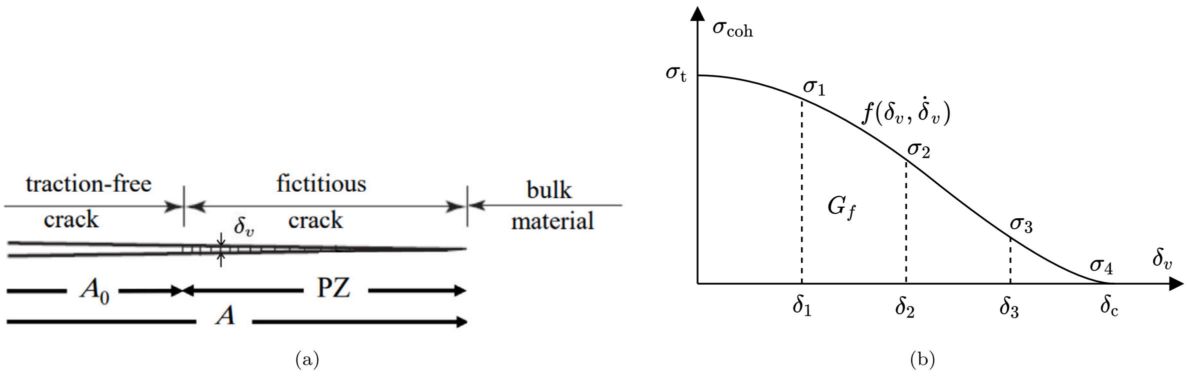

Fig. 2. (a) Illustration of the fictitious crack model. (b) General stress-separation curve describing the PZ behavior.
Source: Adapted from [2].

3. Modeling

3.1. Linear elastic fracture mechanics (LEFM)

Expression for the apparent fracture toughness (K_Q) for the edge loaded, edge cracked rectangular plate (Fig. 1) was derived using the weight function approach [25] in [2] as follows:

$$K_Q = \frac{P_i}{dh\sqrt{L}} \sqrt{\frac{2a_0}{\pi}}\, Z_1(d, a_0) \tag{1}$$

where P_i is the measured load at crack growth initiation, L the crack-parallel side length of the rectangular plate (Fig. 1), $d = D/L$, $a_0 = A_0/L$, and $Z_1(d, a_0)$ is given by Eq. A4 in [2].

3.2. Non-linear viscoelastic fictitious crack model (VFCM)

The VFCM [27] assumes the development of a process zone (PZ) ahead of the traction-free crack tip (A_0, Fig. 2a). The points lying within the PZ first transmit the full tensile strength (σ_t), but then the cohesive tensile stress (σ_{coh}) carried at a particular point within the PZ softens with crack opening (Fig. 2b); until a critical separation (δ_c) is reached and the traction-free crack starts propagating. The VFCM models the stress softening within the fracture process zone by a stress-separation ($\sigma - \delta$) curve (Fig. 2b), with the assumption that the behavior of the bulk material is viscoelastic. The VFCM was coupled with an optimization procedure to match the data from the model and the experiments. Details of the modeling procedure is given in [2]. The main outcomes of this approach is the calculation of the crack profile, process zone size (PZ), and fracture energy (G_f) consumed in each experiment. G_f is measured from the area under the $\sigma - \delta$ curve.

4. Results

Table 1 gives the dimensions of the ice samples together with the control displacement rate (CR), the measured ($L, H, A_0, h, P_i, P_{\mathrm{max}}, P_f,\ t_i, t_{\mathrm{max}}, t_f, \mathrm{CMOD_i}, \mathrm{CMOD_{max}}, \mathrm{NCOD1_i}, \mathrm{NCOD1_{max}}$) and computed ($E_{\mathrm{CMOD}}, K_Q, \dot{K}$) results. The subscripts i, max, f denote the instants of crack growth initiation, maximum/peak load, and complete failure, respectively. These instants can be coincident; for example, failure can happen at the maximum load (see Fig. 3b). P is the applied load, t the time, CMOD and NCOD1 the crack opening displacement at the crack mouth and near the tip, respectively (Fig. 1), E_{CMOD} the short-time modulus calculated from the initial linear part of the measured load–CMOD record and used in the VFCM model. This modulus is lower than the Young's modulus of the material. K_Q is the apparent fracture toughness calculated from Eq. (1), and $\dot{K}$ the loading rate computed by dividing K_Q by the time to crack growth initiation (t_i). The tests "RP7, RP8, …, RP13" are the 2017 tests, and the tests "RP15, RP16, …, RP21" are the 2022 tests.

Table 2 gives the VFCM results: the tensile strength (σ_t), the critical crack opening displacement at crack growth initiation (δ_c), the fracture energy (G_f, Fig. 2b), the process zone size (PZ, Fig. 2a), and the notch sensitivity ratio (σ_n/σ_t); σ_n is the peak nominal tensile stress at the crack tip, given by eq. (A1) in [2] for the current geometry and loading configuration.

Fig. 3a shows the load–CMOD records for the 2022 tests and suggests that in some of the tests the crack growth was intermittent. However, as the VFCM model used does not cover softening, this paper is focusing its analysis up to the onset of crack growth. The maximum data points from the curves are collected and plotted with the corresponding 2017 data in Fig. 3c and Fig. 3d, as a function of the time to reach the maximum load and ice thickness, respectively. As the thickness of the ice increases, the measured maximum load increases. The $P_{\mathrm{max}} - h$ data can be fit nicely with a linear function going through the origin (Fig. 3d). The curves

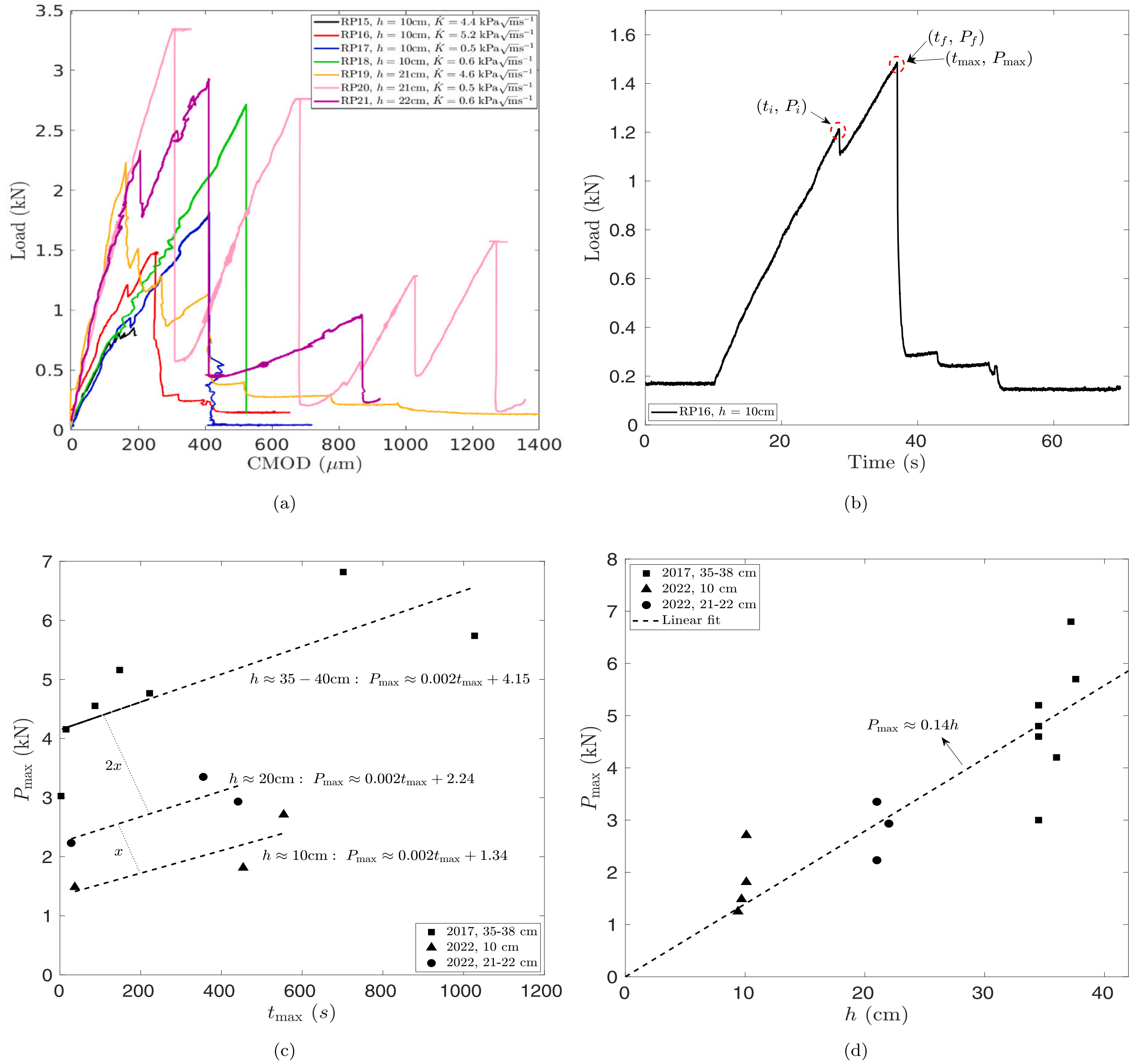

Fig. 3. (a) Load–CMOD records for the 2022 tests. (b) Illustration of the selection of crack growth initiation point (t_i, P_i), maximum point (t_{max}, P_{max}) and failure point (t_f, P_f) for test RP16. Variation of the maximum load as a function of the (c) time to reach the maximum load and (d) ice thickness for all the tests.

of different thickness are parallel to each other (Fig. 3c), indicating that the rate effect can be discussed independently of thickness. The maximum load increases with rate. The distance separating the parallel curves is function of the change in the thickness.

Fig. 4 shows the apparent fracture toughness (K_Q) at the crack growth initiation as a function of loading rate. No thickness effect is detected. The 2017 and 2022 tests' values followed the same rate effect: K_Q decreases as the loading rate increases. The $K_Q - \dot{K}$ relation is non-linear and can be well described with a power-law relation. One data point from the 2022 tests (RP18, 10 cm ice) appears an outlier. The reason for this is not known, but the data is shown here for consistency. Earlier studies have observed similar rate effect on the fracture toughness [6,7,10,12,16]. Gharamti et al. [2] concluded that LEFM is a valid fracture model when $\dot{K} > 50\ \mathrm{kPa}\sqrt{\mathrm{m}}\,\mathrm{s}^{-1}$. From Fig. 4, this corresponds to a fracture toughness of 100 $\mathrm{kPa}\sqrt{\mathrm{m}}\mathrm{s}^{-1}$; this value is considered as the linear elastic fracture toughness of polycrystalline ice [19].

Similarly, Fig. 5 shows the measured values of the crack opening displacement at the crack mouth (CMOD, Fig. 1 and Fig. 5a) and near the crack tip (NCOD1, Fig. 1 and Fig. 5b) at crack growth initiation as a function of loading rate. The thickness had no effect on the crack profile. The rate effect was dominant: CMOD_i and $\mathrm{NCOD1}_i$ values are increasing for longer duration, following almost the same power-law relation.

Fig. 6 displays the fracture energy at crack growth initiation (G_f), calculated from the VFCM (Section 3.2), as a function of the ice thickness and loading rate. No clear thickness effect on the fracture energy values was observed (Fig. 6a). The vertical distribution

Table 1
Specimen dimensions, measured data, and results computed using linear elastic fracture mechanics.

Test	h cm	CR μm/s	E_{CMOD} GPa	P_i kN	P_{max} kN	P_f kN	t_i s	t_{max} s	t_f s	K_Q kPa$\sqrt{m}$	$\dot{K}$ kPa$\sqrt{m}s^{-1}$	CMOD$_i$ μm	CMOD$_{max}$ μm	NCOD1$_i$ μm	NCOD1$_{max}$ μm
RP7	34.5	16.7	6.0	4.6	4.6	4.6	86.9	86.9	86.9	159.4	1.834	236	236	47.2	47.2
RP8	34.5	90.9	6.6	3.0	3.0	3.0	2.7	2.7	2.7	106	39.259	157	157	22.9	22.9
RP9	34.5	16.7	6.1	5.2	5.2	5.2	148.0	148.0	148.0	180.6	1.221	266	266	42.8	42.8
RP10	34.5	4.2	6.7	4.8	4.8	4.8	222.2	222.2	222.2	166.8	0.751	215.6	215.6	34.6	34.6
RP11	36	90.9	7.4	4.2	4.2	4.2	15.3	15.3	15.3	139.4	9.091	174.4	174.4	25.2	25.2
RP12	37.2	3.1	5.7	6.8	6.8	6.8	701.8	701.8	701.8	221.3	0.315	370.5	370.5	68.5	68.5
RP13	37.6	1.7	4.7	5.7	5.7	5.7	1027.1	1027.1	1027.1	184.3	0.179	420.3	420.3	63.4	63.4
RP15	9.4	10	6.0	0.7	1.3	1.3	20.5	–	–	89.6	4.364	112	112	18	18
RP16	9.7	10	6.5	1.2	1.5	1.5	28.4	36.9	36.9	147.9	5.207	166	251	21	37
RP17	10.1	1	5.8	1.8	1.8	1.8	454.0	454.0	454.0	221.1	0.487	412	412	51	51
RP18	10.1	1	6.2	2.7	2.7	2.7	554.3	554.3	554.3	330.7	0.597	522	522	68	68
RP19	21	10	7.6	2.2	2.2	–	28.0	28.0	–	129.6	4.635	162	162	23	23
RP20	21	1	5.9	3.4	3.4	–	355.0	355.0	–	194.5	0.548	308	308	48	48
RP21	22	1	6.3	2.3	2.9	–	228.4	441.3	–	129.1	0.565	205	410	33	82

Table 2
VFCM results.

Test	σ_t (MPa)	δ_c (μm)	G_f (N/m)	PZ (mm)	σ_n/σ_t
RP7	1.30	3.25	4.24	5.9	0.199
RP8	1.24	1.44	1.78	2.7	0.136
RP9	1.32	4.23	5.54	6.4	0.222
RP12	1.02	8.14	8.17	18.4	0.348
RP13	1.00	5.69	5.69	13.2	0.295
RP15	0.91	1.58	2.59	3.8	0.287
RP16	1.30	3.18	11.16	5.6	0.231
RP17	1.21	12.38	8.75	18.1	0.291
RP19	1.00	2.46	6.30	6.5	0.209
RP20	1.26	5.96	10.58	9.8	0.249
RP21	0.80	3.82	5.30	10.3	0.327

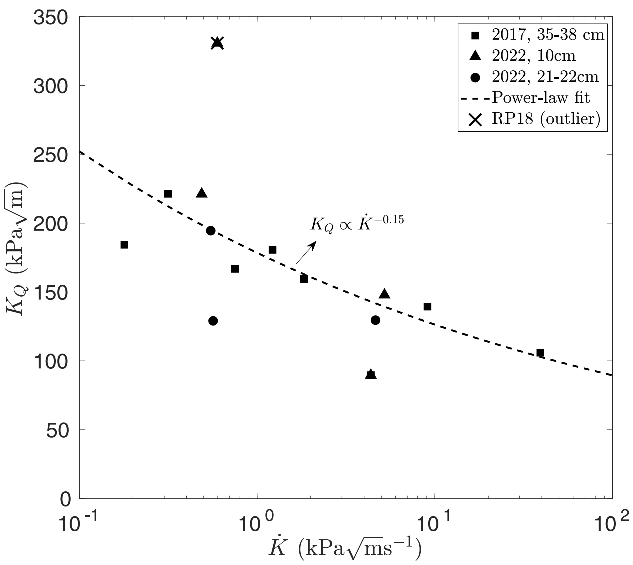

Fig. 4. Variation of the apparent fracture toughness (K_Q) as a function of the loading rate for all the tests. First-order power-law fit was applied to the data.

of each data set represents the rate effect, which can be further seen in Fig. 6b. The G_f values are decreasing with rate. Despite the scatter in the data, it is evident that the data is heading towards an energy value of ≈ 1 N/m under sufficiently high loading rates, resulting in the linear elastic fracture energy of polycrystalline ice [19].

Fig. 7 plots the process zone size (PZ) and critical crack opening displacement (δ_c) at crack growth initiation as a function of loading rate. The PZ size and δ_c values were calculated by the VFCM. The thickness had no clear effect on the PZ and δ_c values; the values were decreasing with rate. Here the process zone is a model parameter and its nature in S2 ice remains an open question.

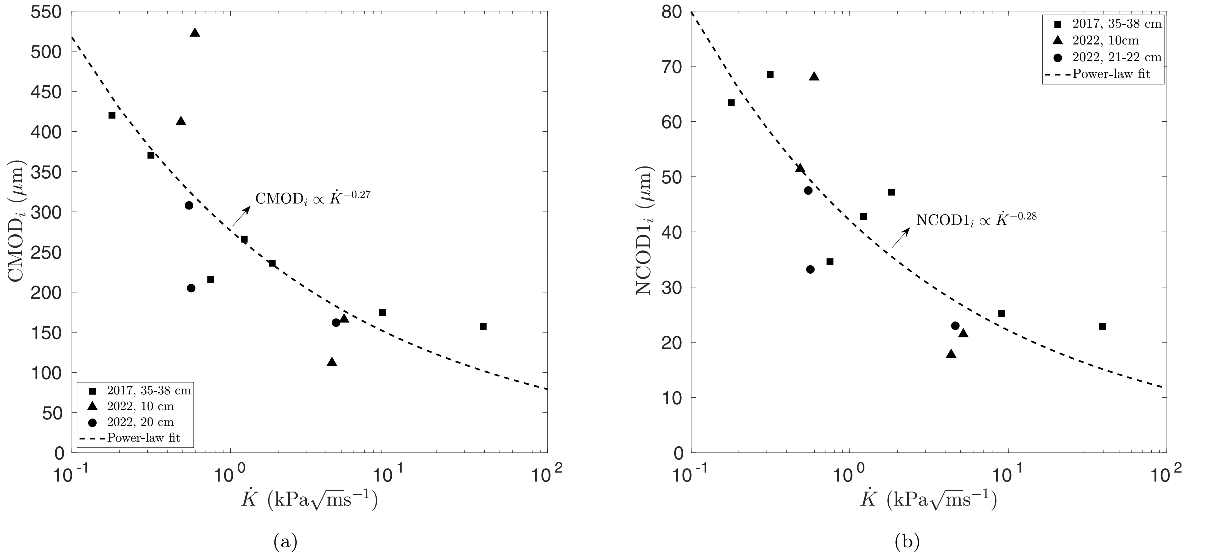

Fig. 5. Measured values of the crack opening displacements (a) at the crack mouth (CMOD) and (b) near the crack-tip (NCOD1) at crack growth initiation as a function of loading rate. First-order power-law fits were applied to the data.

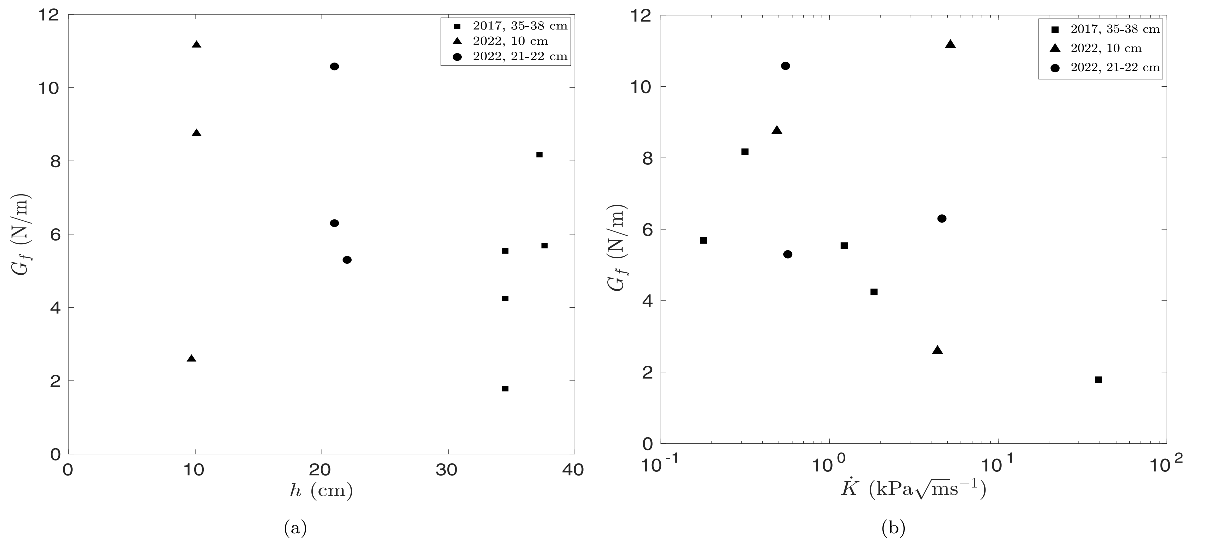

Fig. 6. The fracture energy at crack growth initiation G_f from VFCM as a function of the (a) ice thickness and (b) loading rate.

Fig. 8 plots the notch sensitivity (σ_n/σ_t) as a function of loading rate. Similarly, no thickness effect was observed. The values were in the range 0.2 – 0.4, satisfying the specimen shape-independent fracture condition [2,17].

The reported results indicate that the thickness has no quantitative influence on the fracture properties: the apparent fracture toughness (K_Q), fracture energy (G_f), crack opening displacements (δ_c), process zone size (PZ), and notch sensitivity (σ_n/σ_t).

5. Conclusion

Fourteen Mode I fracture tests were conducted in the Ice and Wave tank of Aalto University in 2017 and 2022. The grown ice was S2 columnar freshwater ice with a warm temperature (> −0.5°C). 3 m × 6 m deep-notched edge-cracked rectangular plates were loaded in displacement control (DC) under different rates monotonically to fracture. The results of the 2022 tests were compared against the 2017 tests to study the effect of the specimen thickness on the ice behavior. The tests covered a thickness variation of $h \approx$ 10–40 cm.

The LEFM was used to compute the apparent fracture toughness, and the VFCM was implemented to model the experiments and compute the fracture energy (G_f), crack profile, and fracture process zone (PZ).

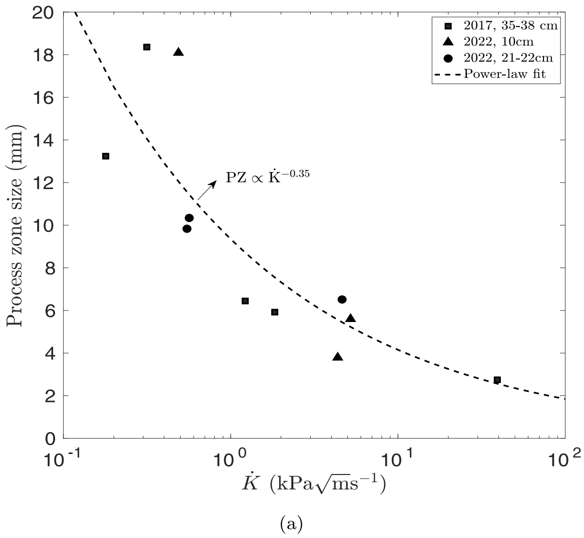

Fig. 7. (a) The process zone size (PZ) and (b) the critical displacement at crack growth initiation (δ_c) as a function of the loading rate.

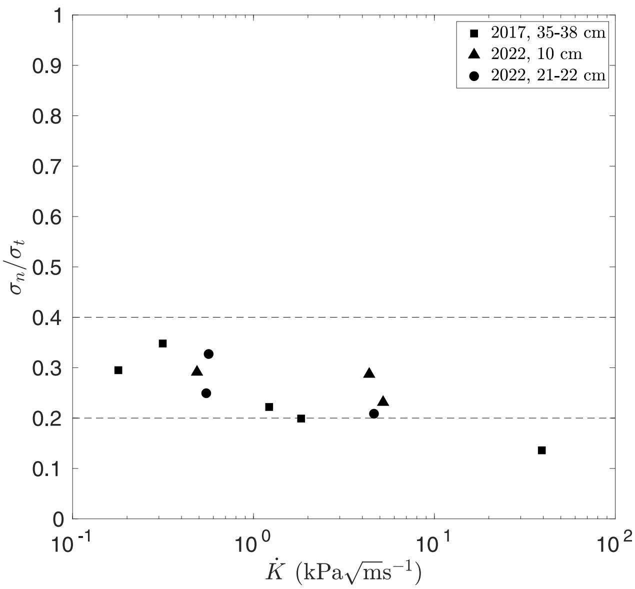

Fig. 8. Notch sensitivity (σ_n/σ_t) as a function of the loading rate.

In light of the results obtained, it is clear that the thickness affected only the values of the measured loads with no influence on the fracture properties: apparent fracture toughness (K_Q), crack opening displacements (CMOD, NCOD1, δ_c), fracture energy (G_f), notch sensitivity (σ_n/σ_t) and process zone size (PZ).

CRediT authorship contribution statement

I.E. Gharamti: Writing – review & editing, Writing – original draft, Methodology, Investigation. **W. Ahmad:** Writing – review & editing, Methodology, Investigation. **O. Puolakka:** Writing – review & editing, Investigation. **J. Tuhkuri:** Writing – review & editing, Supervision, Resources, Investigation.

Declaration of competing interest

The authors declare that they have no known competing financial interests or personal relationships that could have appeared to influence the work reported in this paper.

Data availability

Data will be made available on request.

Acknowledgments

This work was funded by the Academy of Finland through the project Ice Fracture, decision number 351229. The first author (I.E.G) was supported by the Academy of Finland also through the WindySea project (Special 170 RRF funding for research on key areas of green and digital transition [grant number 348588]). This financial support is gratefully acknowledged. The authors would also like to thank Teemu Päivärinta and Lasse Turja for setup design preparation, Kari Hujanen for actuator manufacturing, and Pauli Lehto for comments on the hydraulics and actuator manufacturing.

References

[1] Daley C, Tuhkuri J, Riska K. The role of discrete failures in local ice loads. Cold Reg Sci Technol 1998;27(3):197–211.
[2] Gharamti IE, Dempsey JP, Polojärvi A, Tuhkuri J. Fracture of S2 columnar freshwater ice: Size and rate effects. Acta Mater 2021;202:22–34.
[3] Gharamti IE, Dempsey JP, Polojärvi A, Tuhkuri J. Creep and fracture of warm columnar freshwater ice. Cryosphere 2021;15(5):2401–13.
[4] Gharamti I, Dempsey J, Polojärvi A, Tuhkuri J. Fracture energy of columnar freshwater ice: Influence of loading type, loading rate and size. Materialia 2021;20:101188.
[5] Dempsey JP, Wei Y, DeFranco S, Ruben R, Frachetti R. Fracture toughness of S2 columnar freshwater ice: Crack length and specimen size effects – Part II. In: The 10th international conference on port and ocean engineering under Arctic conditions, vol. 1, Luleå, Sweden; 1989, p. 199–207.
[6] Hamza H, Muggeridge D. Plane strain fracture toughness (K_{1c}) of fresh water ice. In: International conference on port and ocean engineering under Arctic conditions, vol. 1, (no. CONF-790833-):1979, p. 697–707.
[7] Timco GW, Frederking RMW. The effects of anisotropy and microcracks on the fracture toughness (K_{1c}) of freshwater ice. In: Proceedings of the 5th international OMAE symposium, Tokyo, Japan, vol. 4, 1986, p. 341–8.
[8] Bentley DL, Dempsey JP, Sodhi DS, Wei Y. Fracture of S2 columnar freshwater ice: Floating double cantilever beam tests. In: Proceedings of the 9th international IAHR symposium on ice, Sapporo, Japan, vol. 1, 1988, p. 152–61.
[9] Dempsey JP, DeFranco SJ, Adamson RM, Mulmule SV. Scale effects on the in-situ tensile strength and fracture of ice. Part I: Large grained freshwater ice at Spray Lakes Reservoir, Alberta. Int J Fract 1999;95:325–45.
[10] Liu H, Miller K. Fracture toughness of fresh-water ice. J Glaciol 1979;22:135–43.
[11] Timco G, Frederking R. Comparative strengths of fresh water ice. Cold Reg Sci & Technol 1982;6:21–7.
[12] Urabe N, Yoshitake A. Strain rate dependent fracture toughness (K_{1c}) of pure ice and sea ice. In: Proceedings of the 6th IAHR symposium on ice, Quebec city, PQ, Canada, vol. 2, 1981, p. 551–63.
[13] Parsons B, Snellen J, Muggeridge D. The double torsion test applied to fine grained freshwater columnar ice and sea ice. Mech Creep Brittle Mater 1989;1:188–200.
[14] Goodman D, Tabor D. Fracture toughness of ice: A preliminary account of some new experiments. J Glaciol 1978;21:651–60.
[15] Wei Y, DeFranco S, Dempsey JP. Crack-fabrication techniques and their effects on the fracture toughness and CTOD for fresh-water columnar ice. J Glaciol 1991;37:270–80.
[16] Nixon W, Schulson E. Fracture toughness of freshwater ice as a function of loading rate. In: Proceedings of the 1st international conference on ice technology, Cambridge, MA. 1986, p. 287–96.
[17] Dempsey JP. The fracture toughness of ice. In: Ice-structure interaction. Springer, Berlin, Heidelberg; 1991, p. 109–45.
[18] Cole DM. Effect of grain size on the internal fracturing of polycrystalline ice. CRREL report 86-5. USA Cold Regions Research and Engineering Laboratory; 1986.
[19] Schulson E, Duval P. Creep and fracture of ice. Cambridge University Press; 2009.
[20] Abdel-Tawab K, Rodin GJ. Fracture size effects and polycrystalline inhomogeneity. Int J Fract 1998;93(1–4):247–59.
[21] Rodin GJ. On fracture of warm ice. In: IUTAM symposium on scaling laws in ice mechanics and ice dynamics. Springer; 2001, p. 207–16.
[22] Broek D. Elementary engineering fracture mechanics. Leiden: Noordhoff Publishing Co.; 1974.
[23] Hillerborg A. Analysis of one single crack. In: Fracture mechanics of concrete. Amsterdam: Elsevier; 1983, p. 223–49.
[24] Mindess S, Nadeau JS. Effect of notch width on (K_{1c}) for mortar and concrete. Cem Concr Res 1976;6(4):529–34.
[25] Dempsey JP, Mu Z. Weight function for an edge-cracked rectangular plate. Eng Fract Mech 2014;132:93–103.
[26] Mulmule SV, Dempsey JP. A viscoelastic fictitious crack model for the fracture of sea ice. Mech Time-Depend Mater 1997;1:331–56.
[27] Hillerborg A, Modéer M, Petersson P-E. Analysis of crack formation and crack growth in concrete by means of fracture mechanics and finite elements. Cem Concr Res 1976;6:773–81.